

AD744243

NOLTR 72-90

FINITE AMPLITUDE PROPAGATION OF AN
UNDERWATER EXPLOSION SHOCK WAVE
OUT TO A CONVERGENCE-ZONE CAUSTIC

By
John F. Goertner

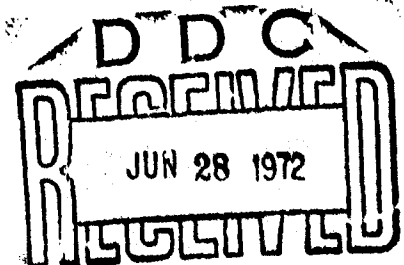
8 MAY 1972

NOL

NAVAL OPDNANCE LABORATORY, WHITE OAK, SILVER SPRING, MARYLAND

APPROVED FOR PUBLIC RELEASE;
DISTRIBUTION UNLIMITED

Reproduced by
NATIONAL TECHNICAL
INFORMATION SERVICE
U.S. Department of Commerce
Springfield, VA 22151



NOLTR 72-90

UNCLASSIFIED

Security Classification

DOCUMENT CONTROL DATA - R & D

(Security classification of title, body of abstract and indexing annotation must be entered when the overall report is classified)

1. ORIGINATING ACTIVITY (Corporate author)		2. REPORT SECURITY CLASSIFICATION	
Naval Ordnance Laboratory White Oak, Silver Spring, Maryland 20910		UNCLASSIFIED	
3. REPORT TITLE		2b. GROUP	
Finite Amplitude Propagation of an Underwater Explosion Shock Wave out to a Convergence-Zone Caustic			
4. DESCRIPTIVE NOTES (Type of report and inclusive dates)			
5. AUTHOR(S) (First name, middle initial, last name)			
John F. Goertner			
6. REPORT DATE	7a. TOTAL NO. OF PAGES	7b. NO. OF REFS	
8 May 1972	iii + 20	6	
8a. CONTRACT OR GRANT NO.	9a. ORIGINATOR'S REPORT NUMBER(S)		
b. PROJECT NO. DNA Subtask NA 002/20	NOLTR 72-90		
c.	9b. OTHER REPORT NO(S) (Any other numbers that may be assigned this report)		
d.			
10. DISTRIBUTION STATEMENT			
Approved for Public Release; Distribution Unlimited			
11. SUPPLEMENTARY NOTES		12. SPONSORING MILITARY ACTIVITY	
		Defense Nuclear Agency Washington, D.C.	
13. ABSTRACT			
<p>The effect of wave overtaking on the peak pressure of refracted underwater explosion shock waves is estimated by a method-of-characteristics calculation. The results show that considerably greater attenuation of the peak pressure occurs as a shock wave travels out to a convergence-zone caustic in the ocean than is experienced by a non-refracted shock wave traveling the same distance. Depending on the explosion conditions, taking account of this additional attenuation can reduce the predicted peak pressure in the vicinity of the caustic by as much as 30%. The report provides a simple method for estimating this effect for particular conditions using routinely available output data from ray tracing programs.</p>			

1a

14

KEY WORDS

LINK A

LINK B

LINK C

ROLE

WT

ROLE

WT

ROLE

WT

Underwater Explosions

Refraction

Shock Wave

Finite Amplitude Wave Propagation

Caustics

Nuclear Explosions

Ray Tracing

Ib

NOLTR 72-90

FINITE AMPLITUDE PROPAGATION OF AN UNDERWATER EXPLOSION
SHOCK WAVE OUT TO A CONVERGENCE-ZONE CAUSTIC

Prepared by:
John F. Goertner

ABSTRACT: The effect of wave overtaking on the peak pressure of refracted underwater explosion shock waves is estimated by a method-of-characteristics calculation. The results show that considerably greater attenuation of the peak pressure occurs as a shock wave travels out to a convergence-zone caustic in the ocean than is experienced by a non-refracted shock wave traveling the same distance. Depending on the explosion conditions, taking account of this additional attenuation can reduce the predicted peak pressure in the vicinity of the caustic by as much as 30%. The report provides a simple method for estimating this effect for particular conditions using routinely available output data from ray tracing programs.

EXPLOSIONS RESEARCH DEPARTMENT
UNDERWATER EXPLOSIONS DIVISION
NAVAL ORDNANCE LABORATORY
White Oak, Maryland

IC

NOLTR 72-90

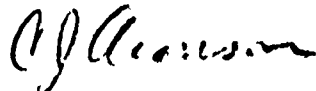
8 May 1972

Finite Amplitude Propagation of an Underwater Explosion Shock Wave Out to a
Convergence-Zone Caustic

Present understanding of the refraction of underwater explosion shock waves has been achieved largely through the use of acoustic theory, i.e., theory of low amplitude pressure waves, with an overall modification to account for explosion pulse propagation. The work reported here is a continuation of a study (reported in NOLTR 71-139) undertaken to determine whether it is necessary to modify the present methods so as to intrinsically incorporate the non-linear effects due to the finite amplitude of explosion pulses. The work was supported by Defense Nuclear Agency Work Unit NA 002/20, Underwater Shock Theory/Energy Focusing and Refraction Effects.

The author is indebted to Robert M. Barash for many valuable suggestions during the course of this work.

ROBERT WILLIAMSON II
Captain, USN
Commander



C. J. ARONSON
By direction

II

CONTENTS

	Page
1. INTRODUCTION.....	1
2. EFFECT OF WAVE-OVERTAKING ON A SHOCK WAVE EN ROUTE TO A CONVERGENCE-ZONE CAUSTIC.....	1
3. VARIABILITY IN WAVE-OVERTAKING EFFECTS.....	6
4. SUMMARY OF RESULTS.....	15
5. DISCUSSION.....	18
6. REFERENCES.....	20

ILLUSTRATIONS

Figure	Title	Page
1	Velocity Profile and Ray Diagram for a Convergence-Zone Caustic.....	2
2	Comparison of Ray Tube Area Functions.....	4
3	Comparison of Enhanced Wave-Overtaking En Route to Convergence-Zone and Thermocline-Related Caustics.....	5
4	Sketch Showing Notation for Bi-Linear Sound Velocity Profiles and Ray Paths.....	8
5	Sketch Showing Bi-Linear Profiles and Source Depths Used for this Study.....	9
6	Sketch Showing Specific Wave-Front Length, L, as a Function of Path Length Along the Ray	12
7	Three Bi-Linear Velocity Profiles and the Corresponding Rays to First Caustic.....	14
8	Comparison of Ray Tube Area Functions from Bi-Linear Velocity Profiles.....	16
9	Comparison of Enhanced Wave-Overtaking -- Bi-Linear Velocity Profiles.....	17

TABLES

Table	Title	Page
1	Comparison of Wave-Overtaking for Two Different Sound Velocity Profiles.....	6
2	Bi-Linear Profile Parameters Estimated from Ocean Sound Velocity Profiles (Naval Oceanographic Office, 1967).....	7
3	Parameters of Rays Calculated from Bi-Linear Sound Velocity Profiles.....	13

FINITE AMPLITUDE PROPAGATION OF AN UNDERWATER EXPLOSION SHOCK WAVE OUT TO A CONVERGENCE-ZONE CAUSTIC

1. INTRODUCTION

An earlier report (Goertner, 1971) developed a computation for the finite amplitude propagation of an underwater explosion shock wave along a tube of varying cross-section. This was a quasi-one-dimensional method-of-characteristics solution which was then used to estimate the effect of wave overtaking (a finite amplitude effect) on the peak pressure of a refracted underwater explosion shock wave en route to a thermocline-related caustic. The "tube" was taken as the ray tube obtained by rotating two adjacent ray paths about the vertical axis through the source. These paths were calculated from the sound velocity profile by simple ray theory. For the particular refraction conditions treated, reductions in the peak pressure, p_{\max} , relative to $F \cdot (p_{\max})_{\text{ISO}}$ up to approximately 5% occurred. (In the preceding, F is the acoustic wave amplitude factor*, and $(p_{\max})_{\text{ISO}}$ is the shock front pressure of a shock wave in isovelocity water at the same path length as the refracted one.) The product $F \cdot (p_{\max})_{\text{ISO}}$ is thus the estimate for p_{\max} obtained from simple ray theory with the additional assumption that the effect of wave-overtaking on p_{\max} of the refracted wave is in the same ratio as for a spherical wave (isovelocity water) having traveled the same distance. In the present report, we will refer to this earlier report as "Part I."

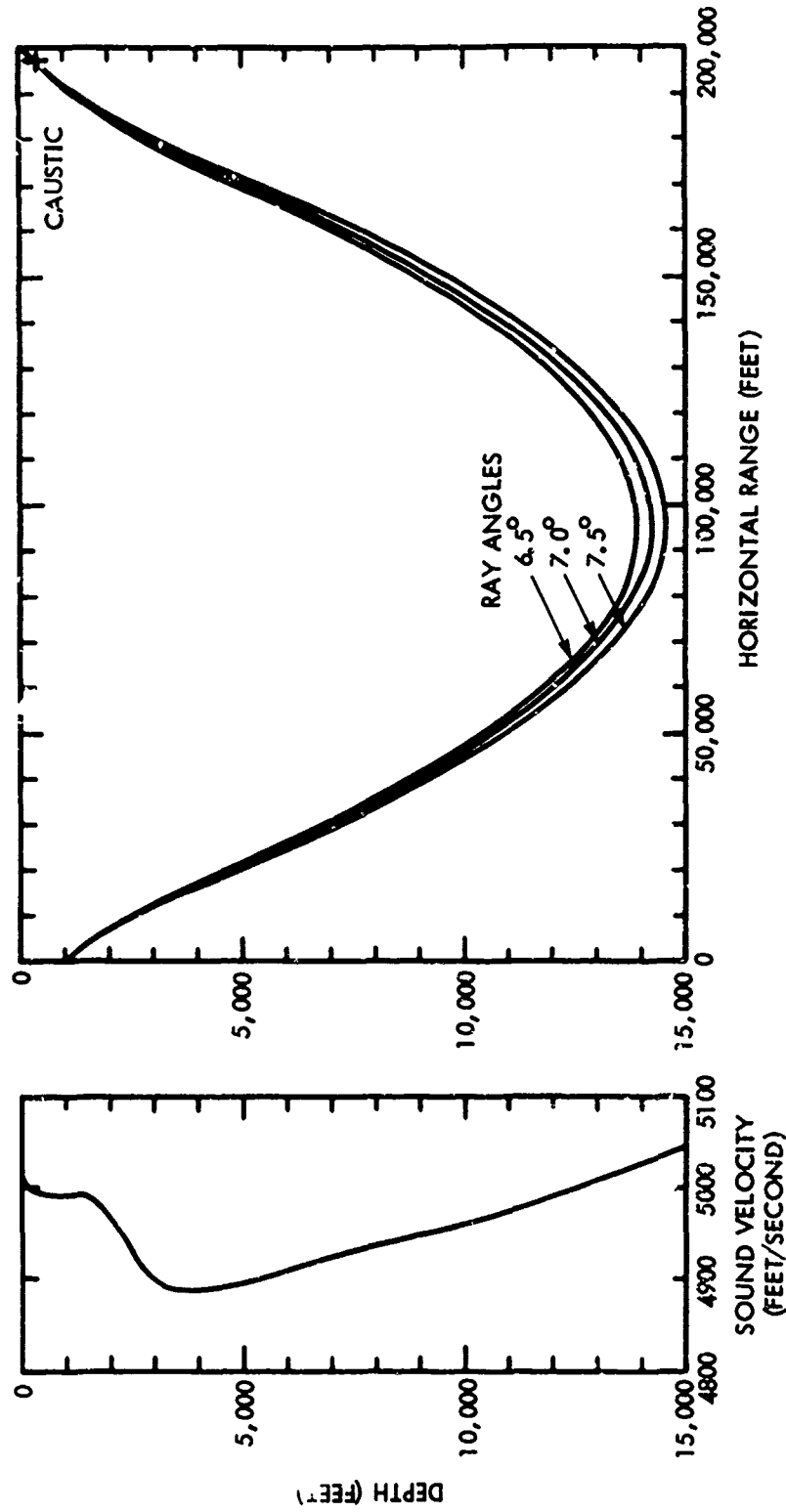
The present report ("Part II" of this study) applies the computation developed in Part I to shock waves en route to convergence-zone caustics in the ocean. It consists of two sections. The first describes a computation carried out for a particular test geometry which corresponds to an earlier ocean experiment. The second describes an attempt to estimate the range of variation in wave-overtaking effects expected to occur due to different weapon employment geometries and ocean environments.

(If the reader is not familiar with Part I, he may wish to read Section 4 of the present report before proceeding to Section 2 and 3, which continue the investigation begun in Part I.)

2. EFFECT OF WAVE-OVERTAKING ON A SHOCK WAVE EN ROUTE TO A CONVERGENCE-ZONE CAUSTIC

Figure 1 shows the measured sound velocity profile and several calculated ray paths taken from the 1966 NOL Sargasso Sea Tests (Blatstein 1971, p 1571). Two adjacent rays out to the first caustic -- those having initial angles of

* The amplitude factor, F , is defined on page 3 by equation 3.



1966 NOL SARGASSO SEA TESTS, PROFILE 21 - SOURCE DEPTH = 1000 FEET
INITIAL RAY ANGLE = 7.0 DEGREES

FIG. 1 VELOCITY PROFILE AND RAY DIAGRAM FOR A CONVERGENCE-ZONE CAUSTIC

$\gamma_0 = 6.5$ and 7.5 degrees -- are shown in addition to the ray of interest, $\gamma_0 = 7.0^\circ$. This section describes the method and results of a computation for the wave propagation along the center ray, $\gamma_0 = 7.0^\circ$.

First, the ray path and wave-front divergence were calculated using a second order numerical integration based on Holl's formulation and analysis of the ray-tracing problem (Holl, 1967, and Holl, 1968)*. In the present report the wave-front divergence is described in terms of Holl's "specific wave-front length"

$$L = \lim_{\Delta\gamma_0 \rightarrow 0} \frac{D}{\Delta\gamma_0} \quad \text{ft/radian} \quad (1)$$

where

D = separation in feet between adjacent rays
 $\Delta\gamma_0$ = initial angular separation of adjacent rays (radians).

Next, we define the "specific wave front area,"

$$A = 2\pi R \bullet L \quad (\text{ft}^2/\text{radian}) \quad (2)$$

where R is the horizontal range in feet from the source. The specific wave-front area is taken as the ray tube cross-section for the calculations of this report. The specific wave-front area defined by equation 2 can be used interchangeably with the ray tube cross-section which was used in Part I -- i.e., $A = 2\pi R \bullet D$ for some suitably small value of γ_0 -- since it is the quantity $\partial \ln A / \partial x$ which governs the wave propagation along the ray tube (Part I, equations 13 and 14). The specific wave-front area for the convergence-zone ray, $\gamma_0 = 7.0^\circ$, shown in Figure 1 is plotted in Figure 2 together with the ray tube cross-section from the ray to a thermocline-related caustic which was calculated in Part I. Figure 2 was obtained by sliding the original log-log plots along the straight (dashed) line representing the initial approximately spherical spreading until the path lengths at the caustics coincided.

The comparison of the effects of wave-overtaking calculated using these two ray tube area functions is shown in Figure 3. In Figure 3, p_{\max} is the calculated peak pressure for the shock front, $(p_{\max})_{\text{ISO}}$ is the calculated peak pressure for the shock front of a spherical wave at a distance from the charge equal to the path length along the refracted ray, and F is the amplitude factor

$$F = \left[\frac{A_0(x)}{A(x)} \right]^{1/2} \quad (3)$$

* Development of this computer program is described in an NOL internal memorandum

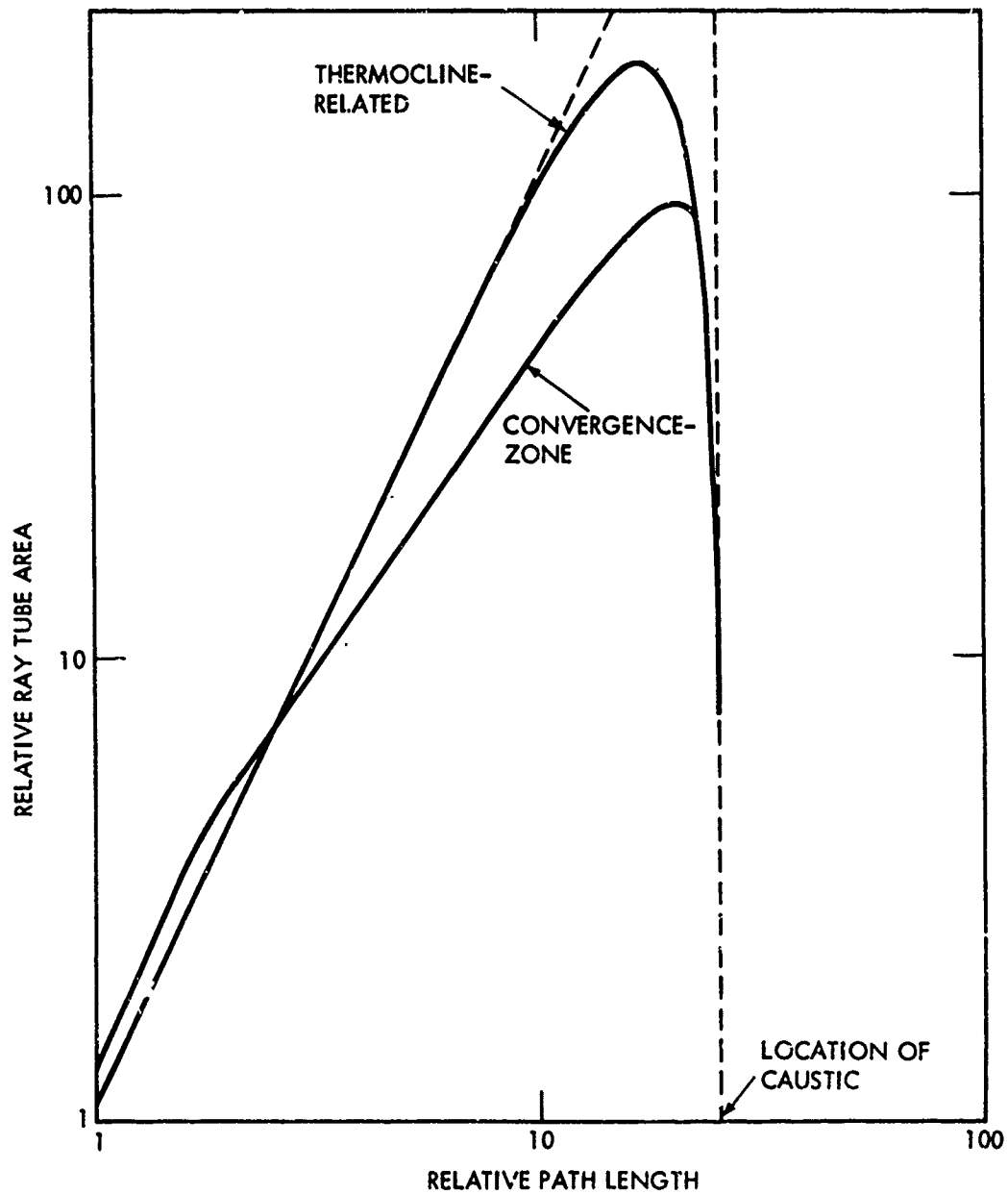


FIG. 2 COMPARISON OF RAY TUBE AREA FUNCTIONS

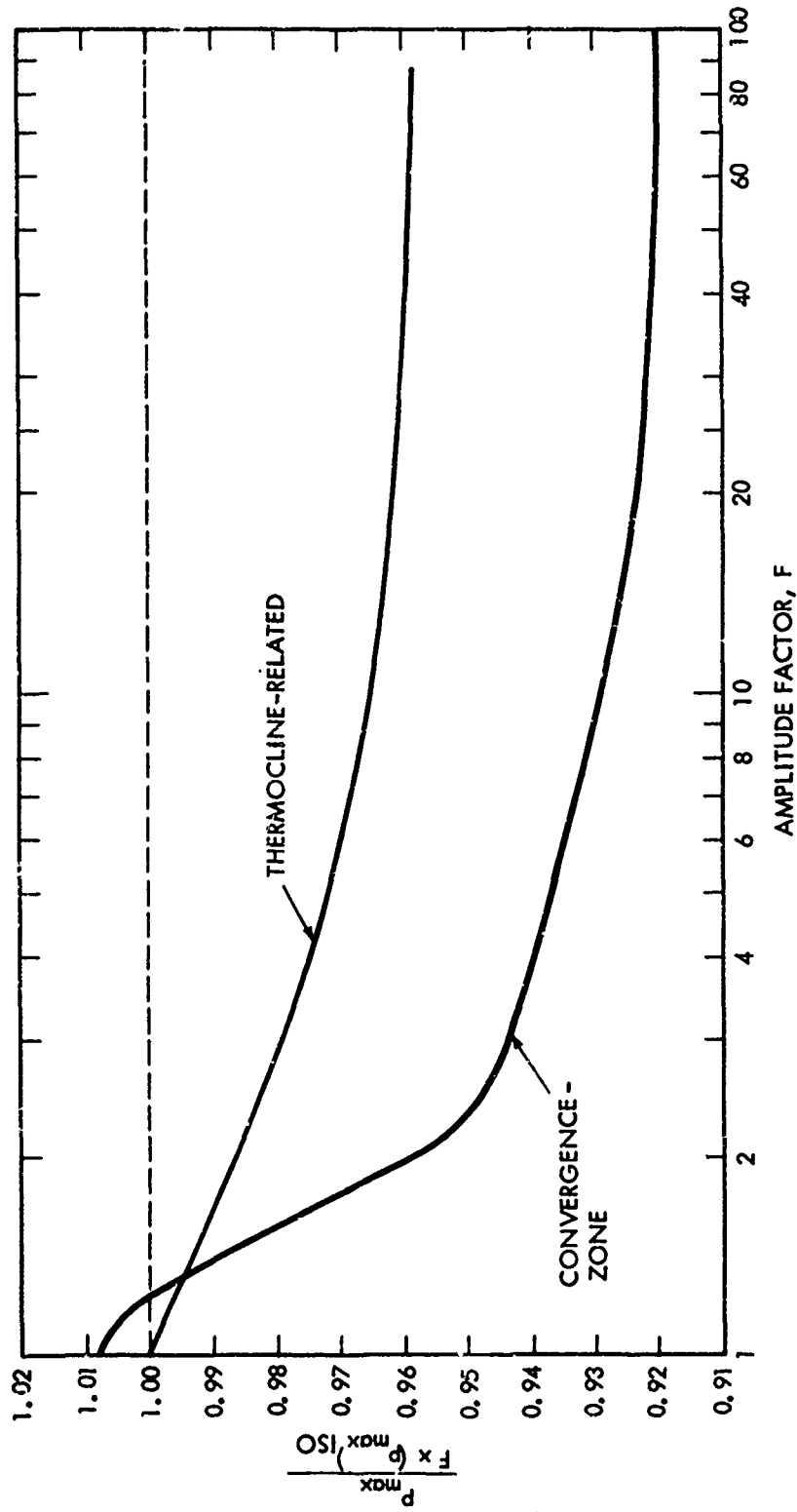


FIG. 3 COMPARISON OF ENHANCED WAVE-OVERTAKING EN ROUTE TO CONVERGENCE-ZONE AND THERMOCLINE-RELATED CAUSTICS

where

$A(x)$ = specific wave front area at distance, x , along the ray
 $A_0(x)$ = specific wave front area for a non-refracted ray at distance, x , from the source

at the particular point along the ray. Both curves were calculated for comparable values of $(p_{\max})_{\text{ISO}}$ at the path length to the caustic*. These values of $(p_{\max})_{\text{ISO}}$ are listed in Table 1 (below) along with values of $\frac{p_{\max}}{F \cdot (p_{\max})_{\text{ISO}}}$, the ratio of the calculated shock front pressure to that predicted by simple ray theory.

TABLE 1

COMPARISON OF WAVE-OVERTAKING FOR TWO DIFFERENT SOUND VELOCITY PROFILES

	$(p_{\max})_{\text{ISO}}$ at Path Length to Caustic (psi)	$\left(\frac{p_{\max}}{F \cdot (p_{\max})_{\text{ISO}}}\right)$ at $F =$				
		2	3	4	6	10
Thermocline-related (Part I)	19	0.987	0.979	0.975	0.970	0.965
Convergence Zone (Present Calculation)	16	0.959	0.944	0.940	0.935	0.929

The percentage correction to p_{\max} -- Figure 3 and Table 1. -- is about twice as large for the ray to the convergence zone caustic as for the thermocline-related caustic described in Part I.

3. VARIABILITY IN WAVE-OVERTAKING EFFECTS

In the previous section we estimated the effect of wave-overtaking on the peak pressure for a single instance of a ray traveling to a convergence zone caustic in the ocean. The effect was much greater than that reported earlier (Part I) for a particular thermocline-related caustic. This led us to investigate the variations which will occur in wave-overtaking effects due to different test geometries and ocean environments.

It was considerably beyond our means to make a statistical study of the infinite set of possible sound velocity profiles and the concomitant variations in the wave-overtaking effects. But, it did seem likely that we could isolate and approximate one or more of the important characteristics (or parameters) of the velocity profiles in regard to wave overtaking, and then calculate their influence on the wave-overtaking phenomenon.

The bi-linear sound velocity profile seemed suitable for this purpose. Typically, the major portion of the ray path to a convergence zone caustic lies in the deep pressure-dependent sound layer where the sound speed varies

* The sensitivity to variation of $(p_{\max})_{\text{ISO}}$ at the caustic is shown for the thermocline-related ray in Part I, Figure 11. This sensitivity was not investigated in the calculations for this report.

approximately linearly with the depth and can be roughly approximated by a linear velocity segment. The ray starts out, however, in the temperature-dependent region in the vicinity of the surface where the sound speed can vary with depth in a complex manner. For this study we approximate this layer also with a linear velocity segment -- one of slope crudely matched to the overall velocity gradient.

Bi-linear Sound Velocity Profiles Selected for this Study.

For this study we were interested in the range of possible wave-overtaking behavior which could occur in operational ocean environments. We selected for this purpose four sound velocity profiles from those reported in the Oceanographic Atlas of the North Atlantic Ocean (Naval Oceanographic Office, 1967).

Estimates for the parameters of bi-linear profiles which approximate these four ocean profiles are listed in Table II below.

TABLE II

BI-LINEAR PROFILE PARAMETERS ESTIMATED FROM OCEAN SOUND VELOCITY PROFILES
(NAVAL OCEANOGRAPHIC OFFICE, 1967)

	λ_1 (Ft/Sec/Ft)	λ_2 (Ft/Sec/Ft)	Z_1 (Ft)	c_1 (Ft/Sec)
Balearic Basin (Mediterranean)	-0.330	+0.017	450	4950
Sargasso Sea* (Western North Atlantic)	-0.069	+0.014	3600	4875
Canary Islands (Tropics)	-0.033	+0.017	4400	4900
Strait of Gibraltar (Eastern North Atlantic)	0.000	+0.017	7000	4900

The bi-linear profile parameters, λ_1 , λ_2 , Z_1 , c_1 , are defined in Figure 4.

Based on Table II we selected the eight combinations of velocity profiles and source depths for our study which are shown by "■" symbols in Figure 5. These were our estimates for a range of probable operational environment conditions.

As a final limitation to the scope of this study, in each case we considered only that ray which converged to its first caustic at the source depth.

* These parameters were obtained from Profile 21 of the 1966 NOL Sargasso Sea Tests (Blatstein, 1971, p 1571).

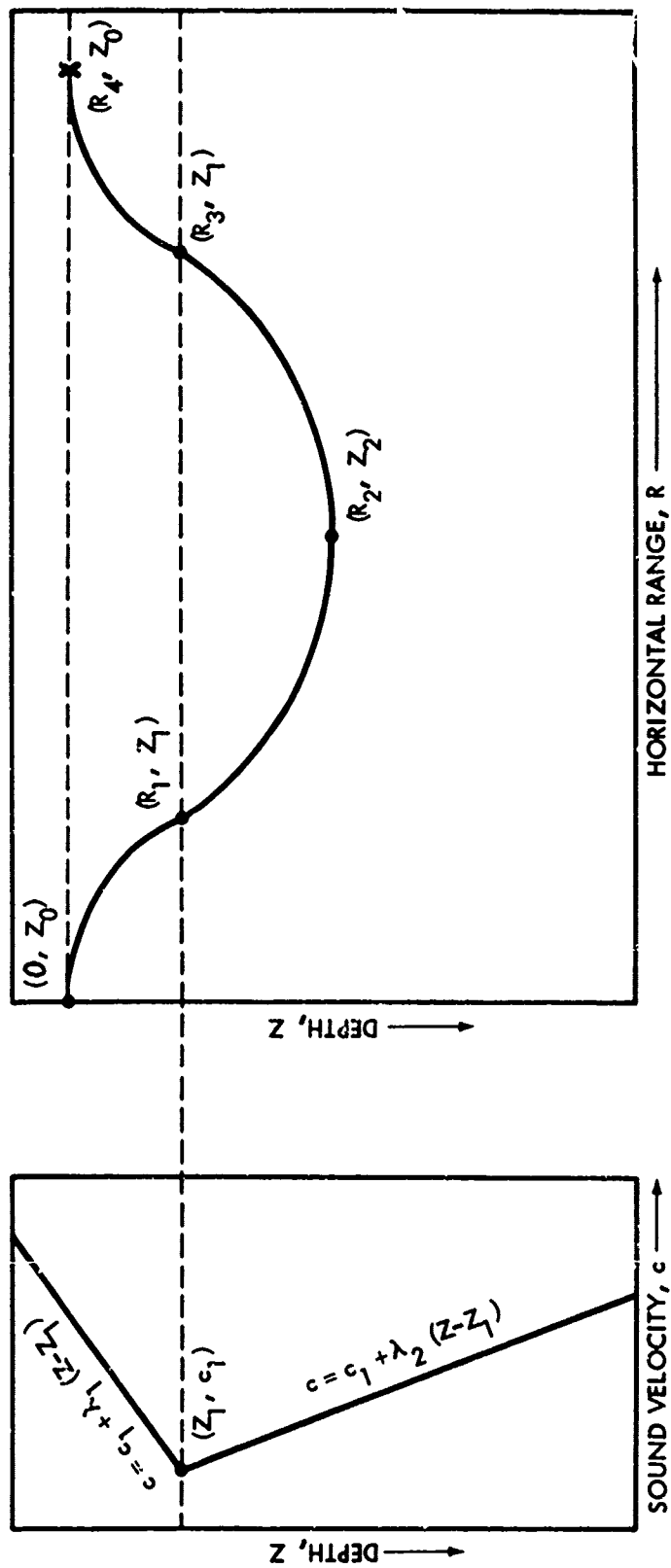


FIG. 4 SKETCH SHOWING NOTATION FOR BI-LINEAR SOUND VELOCITY PROFILES AND RAY PATHS

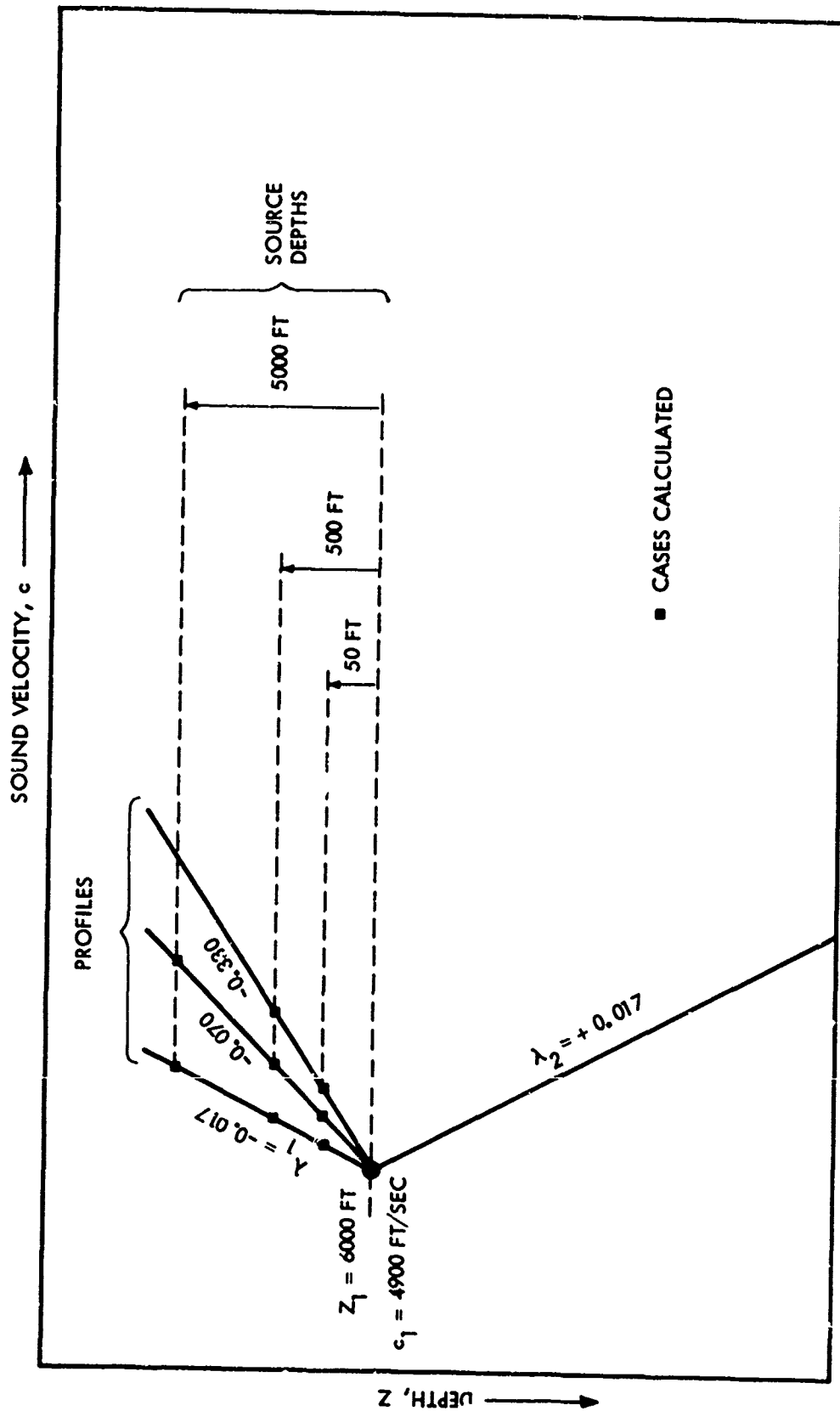


FIG. 5 SKETCH SHOWING BI-LINEAR PROFILES AND SOURCE DEPTHS

Equations for Ray Paths.

The increase in horizontal range, ΔR_i , as the ray traverses the i^{th} layer is given (Spitzer et al, 1948, Chapter 3, equation 84) by

$$\Delta R_i = \frac{c_o}{\cos \gamma_o} \frac{\sin \gamma_i - \sin \gamma_{i+1}}{\lambda_i} \quad (4)$$

where

c_o = sound speed at source depth

γ_o = ray angle at source (measured downward from horizontal)

γ_i and γ_{i+1} = ray angles upon entering and leaving the i^{th} layer

λ_i = constant sound speed gradient, dc/dZ , in i^{th} layer.

Equation (4) was used to calculate required points along the ray trajectory.

In this study we required only the ray with its first caustic at source depth. The range, R_4 , (Figure 4) at which an arbitrary ray returns to source depth is given by a sum of suitable terms from equation (4). To calculate γ_o , the initial ray angle of the ray having a caustic point at range R_4 , we set

$\frac{d}{d\gamma_o} (R_4) = 0$. This gives

$$\tan \gamma_o = \sqrt{\frac{1 - \left(\frac{c_1}{c_o}\right)^2}{\frac{-\lambda_1}{\lambda_2} \left(2 - \frac{\lambda_1}{\lambda_2}\right)}} \quad (5)$$

for the initial angle of the ray having its first caustic at the source depth.

Equations for Wave-Front Divergence.

We describe ray spreading and convergence using Holl's specific wave front length, L . Within the layer having a constant velocity gradient, Holl's differential equation for L (Holl, 1967, Equation 19) reduces to

$$\frac{d\psi}{dx} = \frac{\lambda_i}{c} \psi \sin \gamma \quad (6)$$

where

$$\psi = \frac{dL}{dx} \quad (7)$$

and

x = path length along the ray.

Substituting $c = c_i + \lambda_i (Z - Z_i)$, and $\frac{dZ}{dR} = \sin \gamma$ into (6), and then integrating along the ray inside the i^{th} layer starting at the interface, we derive

$$\frac{dL}{dx} = \psi = \psi_i \frac{c}{c_i} \quad (8)$$

for the rate of change of L along the ray path, where ψ_i and c_i are the upper interface values of dL/dx and the sound speed. Since $dR/dx = \cos \gamma = \frac{c}{c_i} \cos \gamma_i$ (Snell's law), equation 8, expressed in terms of the range, R , simplifies to

$$\frac{dL}{dR} = \frac{\psi_i}{\cos \gamma_i} = \text{constant} \quad (9)$$

inside the i^{th} layer.

The ray angle, γ , as well as L are continuous as the ray crosses the layer boundary. However, there is a jump in γ ($= \frac{dL}{dx}$) at the interface (Holl, 1968, equation 9) given by

$$\Delta \psi_i = \frac{\cos \gamma_o}{c_o} \frac{L}{\tan \gamma} \Delta \lambda_i \quad (10)$$

corresponding to the jump in the sound velocity gradient.

To integrate (9) and (10) along the ray path we note that $L = 0$ and $\psi = \frac{dL}{dx} = 1$ at the source. Figure 6 shows a sketch of L as a function of x for a ray which has its first caustic located at source depth. Note that for this special case L has a constant value ($\frac{dL}{dx} = 0$) in the deep layer. The slopes (dL/dx) of the initial and final segments in the upper layer are $+c/c_o$ and $-c/c_o$, respectively, which for practical purposes is very close to $+1$ and -1 .

Results for Rays Calculated from Bi-linear Profiles.

Using equations (4), (5), (9), and (10) we calculated the ray paths and reduced wave front length for the cases indicated in Figure 5. It turned out that the ratios, L_2/x_4 , (see Figure 6) were almost the same for those cases using the same bi-linear velocity profile. These are tabulated in Table III (below).

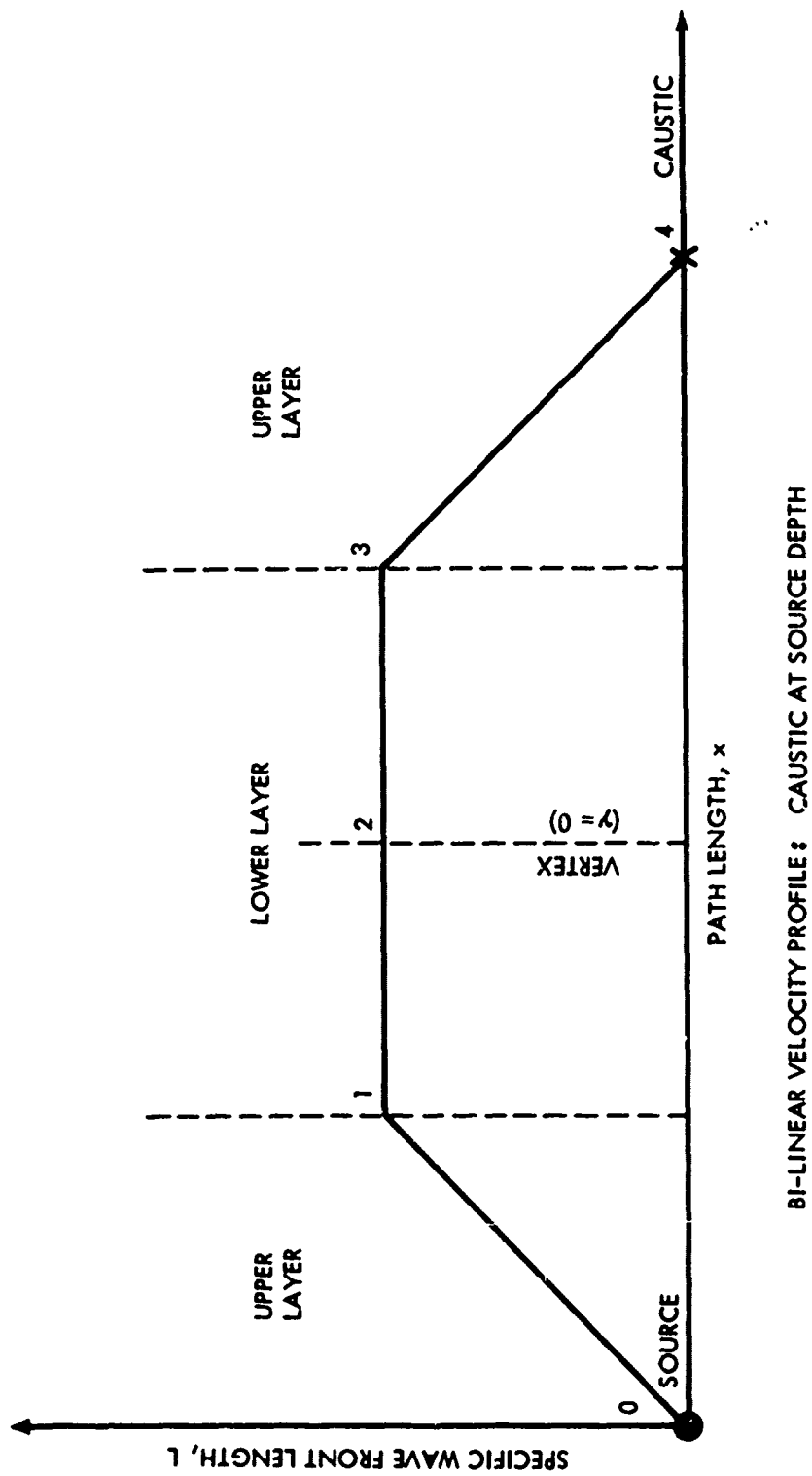


FIG. 6 SKETCH SHOWING SPECIFIC WAVE-FRONT LENGTH, L , AS A FUNCTION OF PATH LENGTH ALONG RAY

TABLE III

PARAMETERS OF RAYS CALCULATED FROM BI-LINEAR SOUND VELOCITY PROFILES

λ_1 (ft/sec/ft)	$z_1 - z_0$ (ft)	x_4 (ft)	L_2 (ft/radian)	L_2/x_4 (radian ⁻¹)
-0.017	50	18,601	3100	0.167
	500	58,894	9812	0.167
	5000	188,556	31,306	0.166
-0.070	50	26,570	2171	0.0817
	500	84,349	6878	0.0816
	5000	276,923	22,147	0.0800
-0.330	50	49,783	1162	0.0233
	500	160,189	3703	0.0231

This means that, to the same approximation, the reduced wave front areas ($A = 2\pi R \cdot L$ ft²/radian) can be scaled to one another in the sense described in Part I (p 11). Thus, in the format chosen for this study of wave-overtaking effects, the eight cases depicted in Figure 5 have been reduced to three, one for each bi-linear velocity profile.*

Paths of the three calculated rays used for this study are plotted in Figure 7 along with the three bi-linear velocity profiles. The source was assumed to be 500 ft above the sound velocity minimum for all three cases. For all three cases the first caustic occurs at the source depth (by design). Figure 8 shows a scaled plot of the wave front areas for the three rays. Note that as the sound speed gradient in the top layer becomes steeper the ray travels a greater fraction of its path in the deep layer where cylindrical spreading occurs. (The spreading turns out to be exactly cylindrical for these bi-linear rays because we selected only those rays going through their first caustic at the same depth as the source. The dashed line shows for comparison the ray tube area function from the Sargasso Sea experiment which was used to calculate the results presented in Section 2. Note this area function is more closely approximated by the $\lambda_1 = -0.017$ curve than by the $\lambda_1 = -0.070$ curve calculated from the bi-linear profile derived from the Sargasso Sea sound velocity measurement. This points up the imperfect nature of these bi-linear fits.

* Note, however, that the path length to the first caustic varied with the source depth. Thus, for example, the scaling of a calculation made for one source depth to another source depth -- same velocity profile -- yields a result which is valid for a scaled (different) charge weight. In other words, by this scaling we have reduced the number of independent variables from 3 -- profile, source depth, charge size -- to 2 -- the profile and the isovelocity pressure level at the caustic.

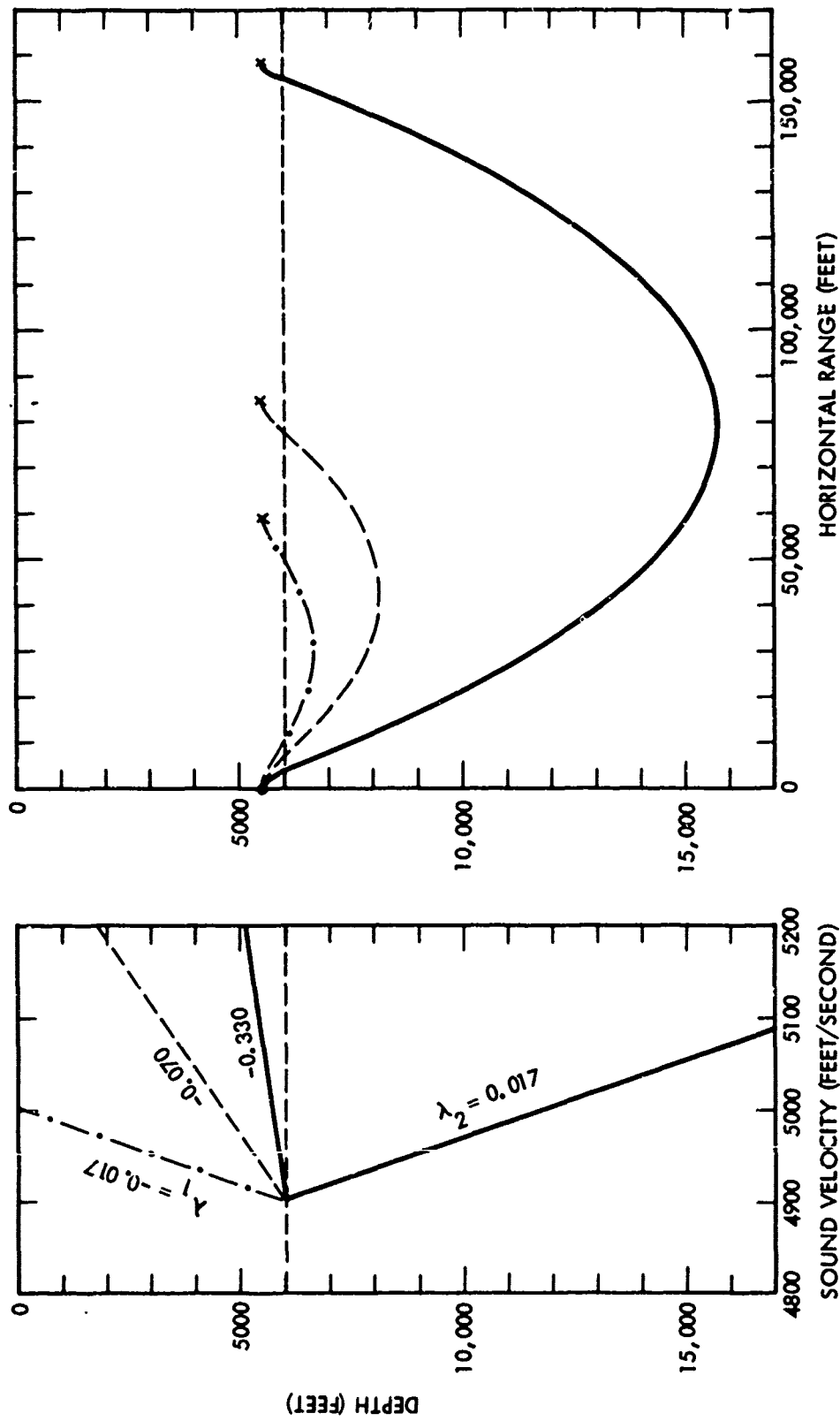


FIG. 7 THREE BI-LINEAR VELOCITY PROFILES AND THE CORRESPONDING RAYS TO FIRST CAUSTIC

For each of the three ray tube area functions shown in Figure 8 we made a method-of-characteristics computation for the finite amplitude wave propagation (as described in Part I). In each case the source TNT charge weight was selected to yield an isovelocity peak pressure of 18.3 psi at the same path length as the caustic. (This corresponds to a 20 kiloton TNT charge with the caustic located at a range of 180,000 feet.)

Figure 9 shows the effect of wave-overtaking on the calculated peak pressure for the three bi-linear profile cases. Note the considerable correction to p_{\max} -- approximately 26% -- for the extreme case, $\lambda_1 = -0.330$ ft/sec/ft. The earlier result obtained using the measured velocity profile from the Sargasso Sea experiment is also shown for comparison (dashed line).

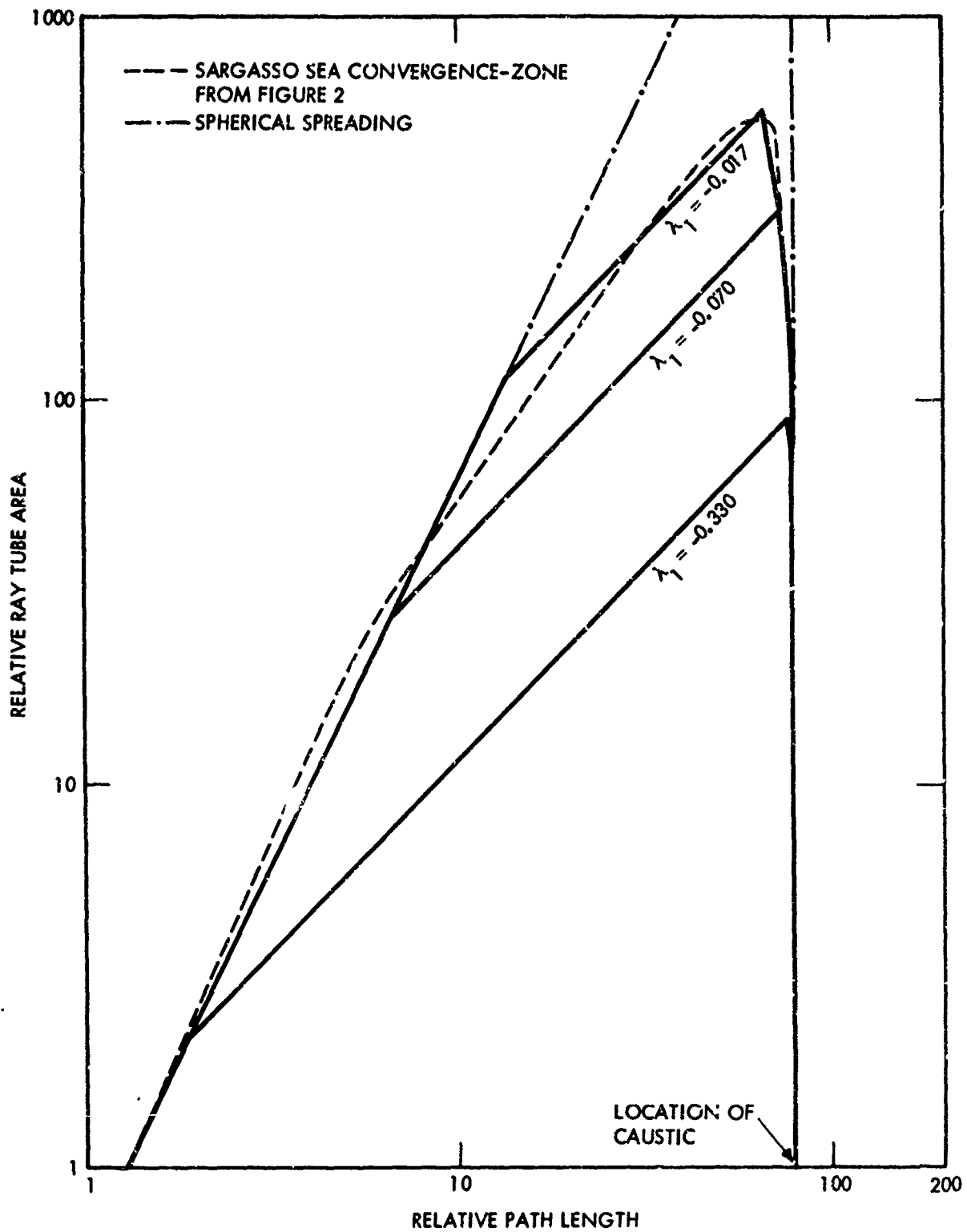
4. SUMMARY OF RESULTS

This report, taken together with the earlier one (Part I), completes a cursory look into the effects of finite amplitude wave-overtaking in refracted underwater explosion shock waves. We started in Part I by considering a sampling of refracted rays calculated from a single measured sound velocity profile which formed a thermocline-related caustic. Two of those rays were rays traveling out to the caustic. For those rays we calculated that enhanced wave-overtaking due to refraction could cause at most a 3 to 4% reduction in p_{\max} (peak pressure at the shock front). The above result pertains to a charge size such that $(p_{\max})_{\text{ISO}}$, the pressure level for a non-refracted shock wave at a range equal to the distance of the caustic, is 15 to 20 psi. This corresponds to a caustic located at a range of 180,000 feet for a 20 kiloton TNT charge. As shown in Part I there is some dependence of the wave-overtaking on $(p_{\max})_{\text{ISO}}$ (or, on the charge size) -- the larger $(p_{\max})_{\text{ISO}}$, the greater the reduction in p_{\max} -- but this dependence was not investigated further in the present report.

In Section 2 of this report we investigated a single ray en route to a convergence-zone caustic using a sound velocity profile measured in the ocean. For this case, enhanced wave-overtaking due to refractive focusing caused a 7% reduction in p_{\max} as the shock wave approached the caustic. A comparison of ray tube area functions for rays calculated from these two different sound velocity profiles (Figure 2) shows that for the convergence-zone ray the enhanced wave-overtaking occurred over a much greater portion of the ray path to the caustic -- roughly 90% as opposed to about 50%.

In Section 3 we took a cursory look at the variability of sound velocity profiles likely to occur in the ocean and into the concomitant variation in ray tube area functions and wave-overtaking for ray paths calculated from those profiles. We restricted our investigation to rays going through a convergence-zone caustic at the same depth as the source.

We selected from an "Oceanographic Atlas" a small sampling of ocean sound velocity profiles which appeared to cover the range of typical and important submarine operating environments (Table I). We then approximated this sampling of oceanic sound velocity profiles with the three idealized bi-linear profiles shown in Figure 5 and calculated the ray paths and ray tube area functions out to



SOUND VELOCITY GRADIENT, $\lambda_2 = +0.017$ (FT/SEC)/FT
 SOURCE LOCATED 500 FEET ABOVE SOUND VELOCITY MINIMUM

8 RAY TUBE AREA FUNCTIONS FROM BI-LINEAR VELOCITY PROFILES

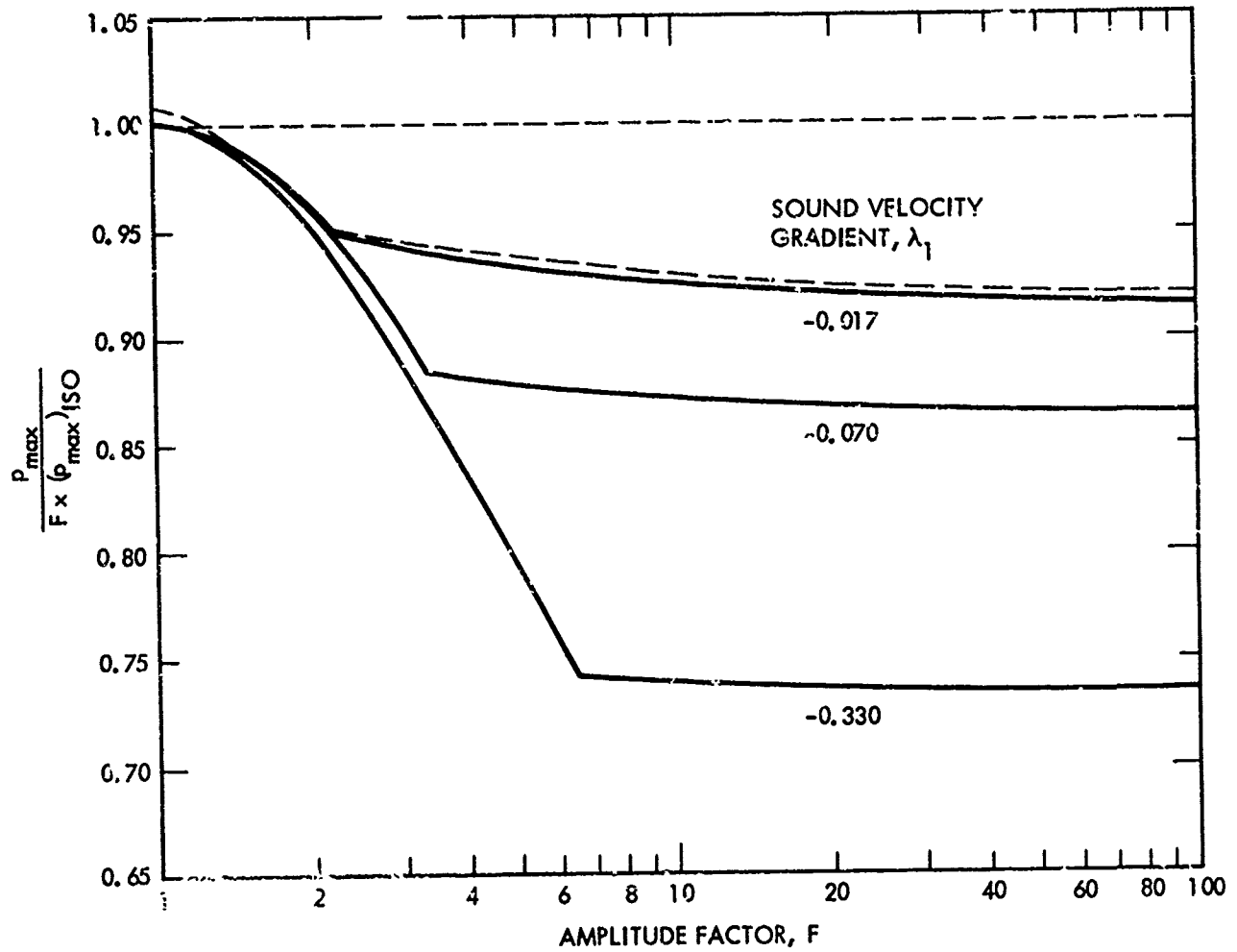


FIG. 9 COMPARISON OF ENHANCED WAVE-OVERTAKING -- BI-LINEAR VELOCITY PROFILES

the convergence-zone caustic for several source depths. For these ray paths to caustics at the same depth as the source, ray tube area functions turned out to be almost invariant with the source depth. The ray tube area functions and the reductions in p_{\max} due to enhanced wave-overtaking calculated using these three idealized profiles are shown in Figures 8 and 9. In addition, the corresponding functions for the convergence-zone ray path investigated in Section 2 are also shown (the dashed lines). From these figures it is apparent that the ray path investigated in Section 2 exhibited minimal enhanced wave-overtaking due to the refraction. The results presented in Figure 9 indicate that we should generally expect the reduction in p_{\max} to be in the range from 7 to 26% as the wave approaches a convergence-zone caustic, depending on the particular ray path and the sound velocity profile.

5. DISCUSSION

It is worth noting that practically all of the reduction in p_{\max} due to refraction-enhanced wave-overtaking occurs as the ray traverses the deep layer. Thus, the wave-overtaking effects we have calculated occur before p_{\max} becomes diffraction-limited (as treated by Blatstein, 1971) in the immediate vicinity of the caustic. For this reason, we have confidence that reductions in p_{\max} such as shown in Figure 9 due to refraction-enhanced wave-overtaking do actually occur in nature.

It is also worth noting that the results plotted in Figure 9 appear well-behaved relative to the input functions, i.e., the ray tube area functions plotted in Figure 8. This is also true for the input functions and results plotted in Figures 2 and 3. Thus, these two pairs of plots provide a simple means of estimating the reduction in peak pressure due to enhanced wave-overtaking for arbitrary ray paths to caustics -- since the area function, or some related quantity, is routinely calculated by most ray tracing programs. One simply plots the area function for the required ray path on the appropriate graph (either Figure 2 or 8) and then makes a corresponding interpolation on either Figure 3 or Figure 9.*

Physical reasoning suggests at least two "finite amplitude effects" contributing to the uncertainty of current results calculated from infinitesimal wave theory:

- (1) An alteration of the shape and amplitude of the wave due to wave-overtaking.
- (2) Errors in the calculated pressures and in the locations of caustics because the equations for refraction and diffraction of a shock wave are not the same as for a sound wave.

In this and the preceding report (Part I) we have attacked and obtained a partial solution to the first of these problems. We found that when finite-

* We would not recommend the alternative approach of making a bi-linear fit to the original sound velocity profile and then either doing a ray tracing calculation for the area function or a direct interpolation of the results shown in Figure 9 using the slope of the upper velocity segment. The bi-linear fit is too crude to do this (see discussion of Figures 7 and 8, page 13, last paragraph).

NOLTR 72-90

amplitude wave-overtaking effects are accounted for, the pressure at a convergence-zone caustic can be up to some 30% lower.

The second problem of "refraction and diffraction of a shock front" (as opposed to a sound wave) appears to be of equal importance. This problem has much in common with the problem of propagation and focusing of sonic booms which has been studied in recent years. It can probably be treated using similar analytic techniques. It should be investigated.

6. REFERENCES

Blatstein, I. M., 1971 J. Acoust. Soc. Am., 49, 1568-1579

Goertner, J. F., 1971, "Finite Amplitude Propagation of an Underwater Explosion Shock Wave Along a Strongly Refracted Ray Tube," NOLTR 71-139

Holl, M. M., 1967, "The Wave-Front-Divergence Factor in Ray Intensity Integration," Meteorology International Incorporated, Project M-140, Contract No. N62271-67-M2000

Holl, M. M., 1968, "The Finite Change in Wavefront Divergence in Passing Through Discontinuities in Sound-Speed Gradient as Effected at Reflections," Meteorology International Incorporated, Project M-143, Contract No. N63134-67-M2854 .

Naval Oceanographic Office, 1967, "Oceanographic Atlas of the North Atlantic Ocean, Section VI--Sound Velocity," N00 Pub. No. 700

Spitzer, Lyman, Jr., et al, 1948 (approx.), "Physics of Sound in the Sea: Part 1: Transmission," Murray Printing Co. (originally issued as a World War II NDRC Summary Technical Report, Division 6 Volume 8)